



LUND UNIVERSITY

Prevention of ischemic myocardial contracture through hemodynamically controlled DCD

Wahlquist, Ylva; Soltesz, Kristian; Liao, Qiuming; Liu, Xiaofei; Pigot, Harry; Sjöberg, Trygve; Steen, Stig

Published in:
Cardiovascular Engineering and Technology

DOI:
[10.1007/s13239-021-00537-8](https://doi.org/10.1007/s13239-021-00537-8)

2021

Document Version:
Early version, also known as pre-print

[Link to publication](#)

Citation for published version (APA):
Wahlquist, Y., Soltesz, K., Liao, Q., Liu, X., Pigot, H., Sjöberg, T., & Steen, S. (2021). Prevention of ischemic myocardial contracture through hemodynamically controlled DCD. *Cardiovascular Engineering and Technology*, 12(5), 485-493. <https://doi.org/10.1007/s13239-021-00537-8>

Total number of authors:
7

General rights

Unless other specific re-use rights are stated the following general rights apply:
Copyright and moral rights for the publications made accessible in the public portal are retained by the authors and/or other copyright owners and it is a condition of accessing publications that users recognise and abide by the legal requirements associated with these rights.

- Users may download and print one copy of any publication from the public portal for the purpose of private study or research.
- You may not further distribute the material or use it for any profit-making activity or commercial gain
- You may freely distribute the URL identifying the publication in the public portal

Read more about Creative commons licenses: <https://creativecommons.org/licenses/>

Take down policy

If you believe that this document breaches copyright please contact us providing details, and we will remove access to the work immediately and investigate your claim.

LUND UNIVERSITY

PO Box 117
221 00 Lund
+46 46-222 00 00

Prevention of ischemic myocardial contracture through hemodynamically controlled DCD

Ylva Wahlquist¹, Kristian Soltesz¹, Qiuming Liao², Xiaofei Liu³, Henry Pigot¹, Trygve Sjöberg² and Stig Steen²

Abstract

Purpose: Ischemic myocardial contracture (IMC) or “stone heart” is a condition with rapid onset following circulatory death. It inhibits transplantability of hearts donated upon circulatory death (DCD). We investigate the effectiveness of hemodynamic normalization upon withdrawal of life-sustaining therapy (WLST) in a large-animal controlled DCD model, with the hypothesis that reduction in cardiac work delays the onset of IMC.

Methods: A large-animal study was conducted comprising of a control group ($n = 6$) receiving no therapy upon WLST, and a test group ($n = 6$) subjected to a protocol for fully automated computer-controlled hemodynamic drug administration. Onset of IMC within 1 h following circulatory death defined the primary end-point. Cardiac work estimates based on pressure-volume loop concepts were developed and used to provide insight into the effectiveness of the proposed computer-controlled therapy.

Results: No test group individual developed IMC within 1 h, whereas all control group individuals did (4/6 within 30 min).

Conclusion: Automatic dosing of hemodynamic drugs in the controlled DCD context has the potential to prevent onset of IMC up to 1 h, enabling ethical and medically safe organ procurement. This has the potential to increase the use of DCD heart transplantation, which has been widely recognized as a means of meeting the growing demand for donor hearts.

Funding

The work was funded by the Swedish government through the Swedish Research Council (grant 2017-04989) and the Hans-Gabriel and Alice Trolle-Wachtmeister Foundation for Medical Research.

Conflicts of interest

The authors have no conflicts of interest to disclose.

Ethics approval

The study ran under ethics permission M174-15, issued by “Malmö/Lunds Djurförsöksetiska Nämnd” (local REB).

Authors' contributions

Study conceptualization: Soltesz, Steen, Wahlquist;

Experimental surgery: Liao, Liu, Steen;

Engineering: Soltesz, Wahlquist;

Data analysis and manuscript: Pigot, Sjöberg, Soltesz, Steen, Wahlquist.

Acknowledgments

The authors would like to acknowledge Zhi Qin with Zhengzhou University, China, for assisting with the study.

¹Wahlquist, Soltesz and Pigot are with the Department of Automatic Control, Lund University, Lund, Sweden. Correspondence to Ylva Wahlquist, E-mail: ylva.wahlquist@control.lth.se

²Liao, Sjöberg and Steen are with the Division of Thoracic Surgery, Department of Clinical Sciences, Lund University, Sweden and the Department of Cardiothoracic Surgery, Skåne University Hospital, Sweden

³Liu is with the First Affiliated Hospital of Zhengzhou University, Zhengzhou, China



(a) Heart without ischemic myocardial contracture.



(b) Heart with ischemic myocardial contracture.

Fig. 1 Transverse sections of two hearts from 35 kg pigs. Heart (a) was procured 1 h after circulatory death, from one of the test group animals; (b) was procured 30 min after circulatory death, from one of the control group animals. Notice that the left-ventricular lumen is almost gone in the contracted heart. Both photos are in the same scale, indicated in (b).

1 Introduction

1.1 Ischemic myocardial contracture

Ischemic myocardial contracture (IMC), commonly referred to as *stone heart*, develops when the myocardium is exerting mechanical work under warm ischemic conditions [1, 2]. The contracture commences at the apex of the heart, and subsequently extends throughout the left heart, before also affecting the right heart. Fig. 1 shows cross sections of (a) one heart without, and (b) one with IMC. The contracture prevents the affected myocardium from performing mechanical work.

During the early era of open-heart surgery using cardiopulmonary bypass, IMC was identified as a rare, but fatal condition [1]. Since it is associated with a loss of perfusion of the affected myocardium, the condition can typically not be reversed, as it prevents transport of required pharmacological substances to the affected site. Several works [3, 4] have investigated preventive measures. Administration of β -blockers, calcium antagonists and regional hypothermia, have all been shown to significantly reduce the risk of IMC [1, 2].

The advent of modern cardioplegia and general methodology development within cardiopulmonary bypass surgery have resulted in fewer instances of IMC. Consequently, the research interest in prevention of ischemic myocardial contracture has also decreased over the last three decades.

1.2 Controlled donation upon circulatory death (DCD)

The inability to meet the demand of transplantable solid organs through donation upon brain death (DBD) from heart-beating brain-dead donors, has led to the reintroduction of donation upon circulatory death (DCD) in several legislations [6, 7]. Ischemic damage, resulting in graft failure, is the main medical concern associated with DCD transplantation [8, 9]. Procurement of DCD hearts is therefore performed under tight temporal constraints, and with maximal effort spent to prevent ischemic myocardial damage [9, 10]. This has limited its clinical application to Maastricht category III donors [11]. This category constitutes in-hospital patients, where a decision to end life-sustaining ventilator support is based on the best interest of the patient.

As opposed to the determination of brain death, there exist no universally accepted criteria for the determination of circulatory death. Instead, its definition relies on the concepts of cessation and irreversibility of cardiopulmonary function [12]. This has resulted in substantial DCD protocol variations between centres [6].

The course of events following withdrawal of life-sustaining therapy (WLST), that all clinical protocols have to relate to, is illustrated in Fig. 2. The time between WLST and death is referred to as the agonal phase. The

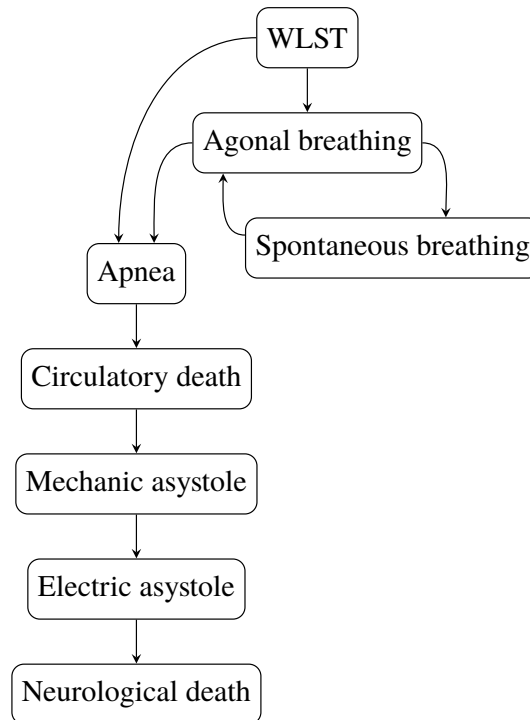


Fig. 2 The course of events following withdrawal of life-sustaining therapy (WLST). Contemporary protocols prevent DCD donation where prolonged episodes (hours to days) are spent in the right cycle. However, such cases are rare, with circulatory death occurring within 2 h in over 70 % of cases [5]

possibility of (short-term) survival [5], illustrated by the right cycle in Fig. 2, imposes legal and ethical restrictions on admissible treatments during, and leading up to, the agonal phase. Particularly, *ante-mortem* interventions should be motivated by the best interest of the patient and must not interfere with the possibility of (short-term) survival.

Measures for organ optimization mainly translate into reducing warm ischemic time. For heart organs, a distinction is made between warm ischemia in asystole and functional warm ischemia [6], where the greater metabolic needs of the latter make it more problematic in the DCD context.

1.3 Hemodynamic control in DCD

The onset of the agonal phase is typically associated with a catecholamine “storm”, resulting in increased systemic resistance, and leading up to relative hypertension, possible tachycardia, and thus an increase in myocardial metabolism [13]. Control of hemodynamic parameters is a potentially viable means of postponing the onset of IMC, and warm ischemic damage in general. Hemodynamic parameters available for pharmacological control include:

- vascular resistance (through arterial and venous tone);
- heart rate;
- myocardial contractility.

Cardiac output and tissue perfusion are directly dependent on the above three parameters. In this study we control these parameters with the goal of facilitating cardiac output after WLST, while limiting the associated cardiac work to avoid episodes of relative hypertension, tachycardia, and ischemia-induced ventricular fibrillation (VF). In this nominal work, we investigate whether the proposed methodology can serve to postpone the onset of ischemic myocardial contracture in a DCD large animal model.

Treatment associated with WLST needs to be delivered with dignity. To meet this need and the critical timing requirements imposed by the scenario, we have developed and demonstrated a fully automated feedback control system, in which a computer administers the delivery of intravenous drugs. The system adjusts the individual dosage of drugs in real-time based on the patient’s hemodynamic response, thus avoiding over- or under-dosing.

2 Methods

2.1 Cardiac work estimation

The hypothesis underlying the study is that the time between WLST and incidence of IMC is correlated with the ischemic work of the heart following WLST. To investigate this hypothesis, one under-estimating approximation

$$\underline{W} \propto \int_0^T P_{sys}(t) HR(t) dt, \quad (1)$$

and one over-estimating approximation

$$\bar{W} \propto \int_0^T P_{sys}^2(t) HR(t) dt, \quad (2)$$

of cardiac work were used where $t = 0$ and $t = T$ denote the instances of WLST, and asystole or VF instance, respectively. P_{sys} is the instantaneous systolic aortic pressure and HR is the instantaneous heart rate, defined at the instances of systolic peaks as $1/\Delta t$, where Δt is the time passed since the preceding systolic peak. See Supplementary Sect. S1 for further details.

2.2 Hemodynamic control

We have developed and evaluated a feedback control system based on a computer-controlled infusion pump array; real-time invasive arterial pressure acquisition system; and a PC running software for measurement, control, actuation, logging, and associated graphical user interface. The base hardware has been described in previous works [14, 15].

The overall objective of the control system was to normalize vascular resistance between the instance of WLST and the incidence of circulatory collapse, defined in Sect. 2.3, in order to facilitate cardiac output while limiting the amount of associated cardiac work. Individualized administration of the drugs is necessary to safely account for the variation in hemodynamic response between individuals after WLST. This motivates computer-controlled real-time adjustment of the timing and number of doses administered according to systolic aortic pressure measurements as opposed to using a fixed bolusing protocol. From prior research [15], we have established the feasibility of normalizing systolic pressure using closed-loop computer control of noradrenaline and nitroglycerine. Nitroglycerine dosing was used as the control signal to decrease vascular resistance. Both bolus and continuous infusion dosing were considered in pilot experiments. It was concluded that bolus dosing was necessary to achieve sufficiently fast responses in P_{sys} . Based on pilot experiments described in Supplementary Sect. S4, the bolus size was set to 1.5 mg.

Pilot experiments indicated tachycardia and tolerance effects when exceeding three nitroglycerine boluses following WLST. If these were not sufficient to establish normotension, subsequent boluses of a synergistic calcium antagonist (nimodipine) and β -blocker (esmolol) mixture, comprising of nimodipine and esmolol, were administered. While counteracting both hypertension and tachycardia, the response time is slower, and the peak effect lower, compared to the nitroglycerine boluses.

Ventricular fibrillation was identified as the main contributor to IMC in our pilot experiments. To prevent this, a lidocaine bolus was given at the time of circulatory death, defined in Sect. 2.3. A bolus dose of the calcium antagonist and β -blocker mixture were administered together with the lidocaine to prevent a prolonged episode of low-intensity myocardial work following circulatory death. The timing and doses of all drugs used in hemodynamic control are given in Supplementary Tab. S1 and S3.

A noradrenaline “safety” feedback controller was implemented for automatic drug infusion to counteract potential overdosing of nitroglycerine, otherwise resulting in hypotension. Systolic aortic pressure responses to constant noradrenaline infusions were recorded in three pilot experiments, and are shown in Supplementary Fig. S4.

Time-delayed first-order linear differential equation models were identified from the noradrenaline infusion responses shown in Supplementary Fig. S4, by minimizing the output error \mathcal{L}_2 norm. A proportional-integral-derivative (PID) controller was optimized for robust performance across these models. The optimization objective was to minimize the time from hypotension due to overdosing of nitroglycerine until acceptable systolic aortic blood pressure values were reached. A step disturbance was used to model the effect of nitroglycerine on the systolic aortic pressure. In the controller optimization, constraints were imposed to enforce robustness over the model set. More details of the controller design can be found in Supplementary Sect. S5.

To attenuate high-frequency measurement noise, a second-order low-pass filter was connected in series with the controller, resulting in the Laplace domain representation

$$K = CF$$

$$C(s) = k_p + k_i \frac{1}{s} + k_d s \quad (3)$$

$$F(s) = \frac{1}{(sT_f + 1)^2}$$

where C is the PID controller, F is the low-pass filter and s is the Laplace variable. The PID parameters were $k_p = 9.63 \cdot 10^{-4}$ mg/h/mmHg, $k_i = 2.96 \cdot 10^{-5}$ mg/h/mmHg/s, $k_d = 8.14 \cdot 10^{-3}$ mg/h/mmHg·s and $T_f = 2$ s. The controller was implemented with clamping anti-windup on the PC used in data acquisition and drug delivery actuation.

The set-point of this noradrenaline “safety” controller was set to 70 mmHg for P_{sys} during the first 3 min following WLST, whereafter the controller was automatically deactivated.

2.3 Experimental study

The primary end-point was to study IMC occurrence 60 min after circulatory death. The secondary end-point was the time between circulatory death and observed IMC.

Equal control and test group sizes of $n = 6$ each were determined, based on 70% anticipated 60 min IMC incidence in the control group, and 0% in the test group, at a false positive rate $\alpha = 0.05$, and false negative rate $\beta = 0.2$ (i.e., 80% power). Inclusion criteria for both groups were defined to facilitate comparability of outcomes: stable hemodynamics at the time of WLST, with $P_{sys} \leq 110$ mmHg and $HR \leq 110$ min⁻¹; absence of agonal breathing following WLST; adherence to drug dosing protocol of the study; absence of anomalies at dissection. Details about animals excluded from the study and conducted pilot cases can be found in Supplementary Sect. S2.

Anesthesia was induced through intravenous injection of atropine, xylazine, and ketamine. Subsequently, midazolam and rocuronium were intravenously administered before placement of an endotracheal tube through tracheostomy. The animals were then mechanically ventilated using volume-controlled and pressure-regulated ventilation.

Upon introduction of intravenous propofol anesthesia, and intubation, the animals were instrumented with transducers to measure arterial and venous blood pressure and a 5-lead ECG. Arterial blood gas samples were collected and analyzed at baseline, and 1, 2, ..., 5 min following WLST. The animals were given heparin to prevent coagulation. Doses and further details on the drugs are provided in Supplementary Sect. S3.

A neuromuscular blockade was established to prevent agonal breathing, whereupon WLST was performed. If the heart rate exceeded 110 bpm between WLST and circulatory collapse, a bolus of esmolol and nimodipine was given. Circulatory collapse was defined to occur at the first incidence of $P_{sys} < 40$ mmHg. Circulatory death (cessation and irreversibility of cardiopulmonary function [12]) was defined as persistent circulatory collapse combined with arterial saturation remaining below $s_aO_2 = 30\%$. Previous studies [9, 16] have associated a systolic pressure fall beneath 50 mmHg with severe ischemia, motivating the choice of the lower systolic pressure limit. By this time, the animals was hypoxic with an arterial oxygen saturation well below 30% [16]. Following a hands-off time of 30 min, sternotomy was performed, and the heart was inspected and palpated for IMC every 5 min until 60 min had passed since circulatory death. If there were palpable and visible signs of contracture in the left ventricular wall, IMC was confirmed. When IMC was verified or when 60 min had passed since circulatory death, the heart was excised and transversely cut into slices as shown in Fig. 1. The heart was then dissected to inspect for anomalies that could have affected the outcome. To complement the qualitative diagnostic assessment with a quantitatively comparable measure, the left ventricular wall thickness was measured as the average thickness within a transverse plane halfway between the atrial-ventricular plane and the apex.

The test and control group protocols were identical with the exception of the test group being subjected to the hemodynamic control protocol described in Sect. 2.2. The test group protocol is illustrated through the flowchart in Fig. 3. Drugs used in the test group protocol were nitroglycerine, noradrenaline, lidocaine, esmolol and nimodipine, see Fig. 3 and Supplementary Tab. S1 and S3 for details about bolus dosing and timing. Noradrenaline was administered by the aforementioned “safety” feedback control system using an Alaris TIVA infusion pump. Bolus doses of the other drugs were manually administered, due to a lack of remote-controlled bolus capability of the Alaris TIVA pumps. This was later implemented, and two additional fully automated cases, one illustrated in Fig. 4, were successfully completed.

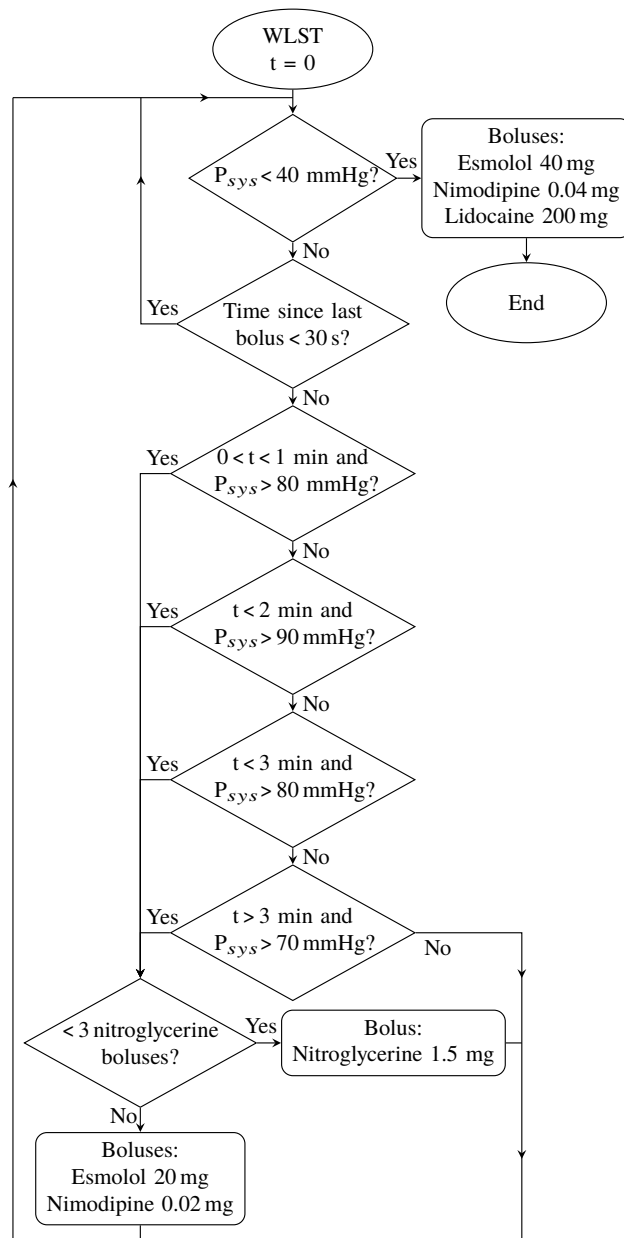


Fig. 3 Flow chart illustrating the test group protocol. Time $t = 0$ starts at the instance of WLST. The noradrenaline “safety” controller is activated during the first 3 min following WLST, in order to avoid hypotension in case of low nitroglycerine tolerance. If the heart rate exceeded 110 bpm between WLST and circulatory collapse, an additional bolus of esmolol and nimodipine was given.

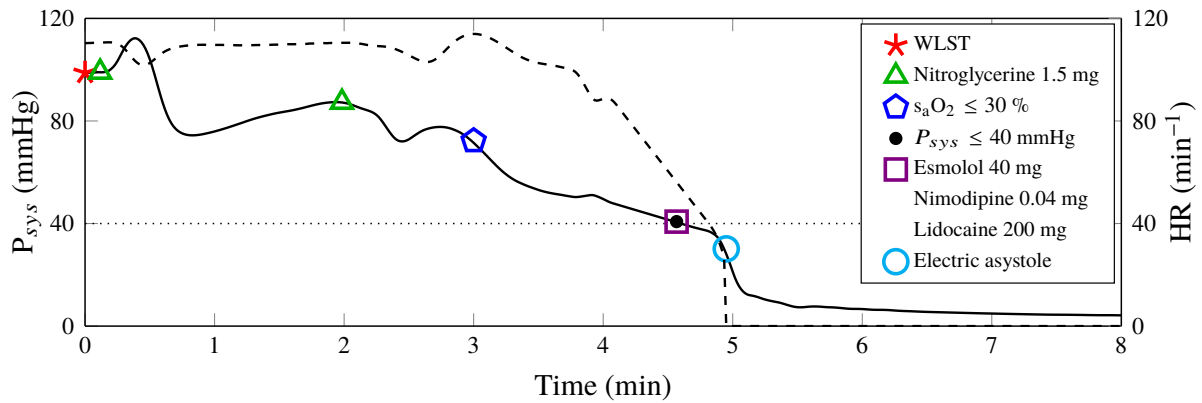


Fig. 4 Representative test group experiment with fully automated drug dosing according to the protocol illustrated in Fig. 3. Systolic pressure, P_{sys} is shown solid and heart rate, HR , in dashed. Markers indicate events according to the figure legend. The dotted black line indicates the systolic pressure associated with circulatory collapse

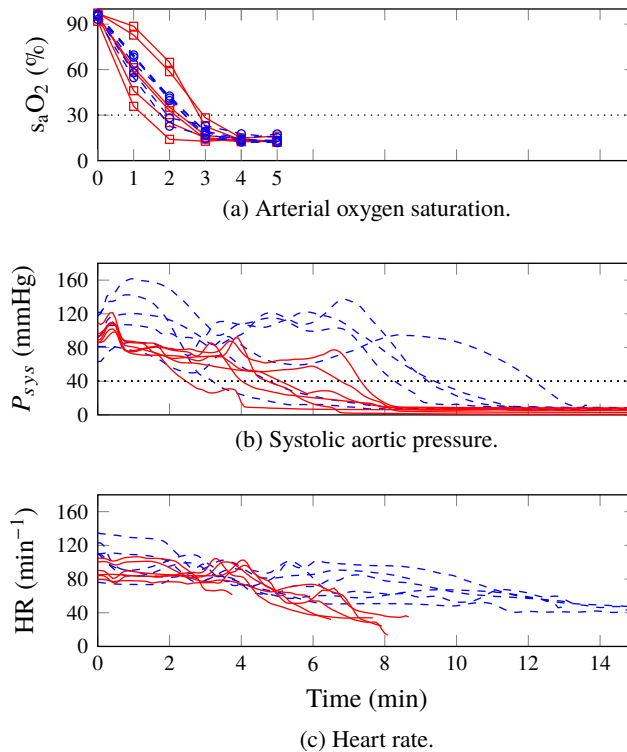


Fig. 5 Test (solid red, squares) and control (dashed blue, circles) group hemodynamic responses following withdrawal of life-sustaining therapy (WLST) at time 0 min. The dotted horizontal line in (a) indicates oxygen saturation $s_aO_2 = 30\%$. The dotted horizontal line in (b) indicates the systolic aortic pressure, $P_{sys} = 40$ mmHg, associated with circulatory collapse. Circulatory death was defined to occur when both $s_aO_2 < 30\%$ and $P_{sys} < 40$ mmHg were fulfilled.

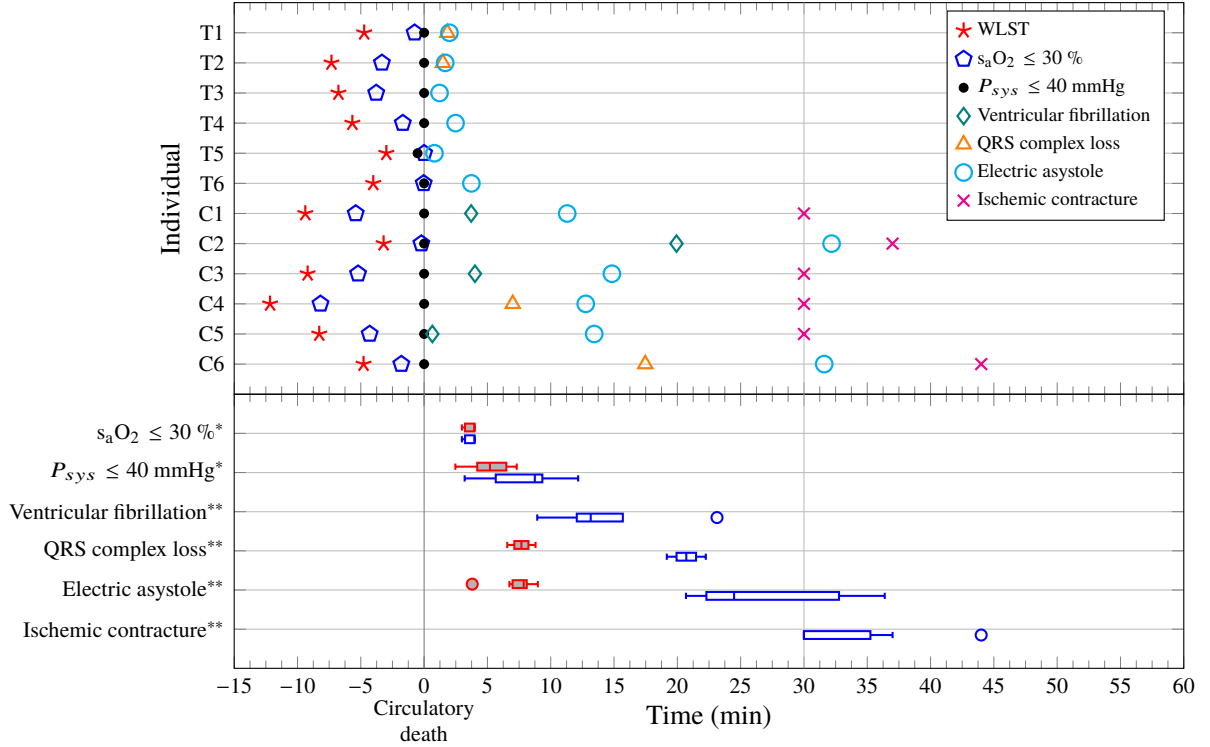


Fig. 6 Distribution of events. The top part shows events for test (T) and control (C) group individuals. QRS complex loss markers have been omitted for individuals where QRS complex loss coincided with ventricular fibrillation or electric asystole. IMC incidence has been reported as 30 min if IMC was observed at the instance of sternotomy, which was performed 30 min after circulatory death. The bottom part shows the distribution of events within the study groups. Filled red boxes are used for the test group; empty blue ones for the control group. In absence of incidence, IMC and ventricular fibrillation statistics are not presented for the test group. Note that the distributions of arterial saturation $s_aO_2 < 30\%$, and systolic pressure $P_{sys} < 40$ mmHg, are reported with the withdrawal of life-sustaining therapy (WLST) time instance as zero reference, while all other events are reported with the time instance of circulatory death as zero reference.

3 Results

The investigated method for normalization of hemodynamics upon WLST with the aim to facilitate DCD procurement of hearts resulted in none of the six test group individuals developing IMC within 60 min of warm ischemia following circulatory death. All six control group individuals developed IMC within 60 min, with four having developed IMC by the time of sternotomy, 30 min following circulatory death.

Fig. 1 shows representative cross sections of two hearts from the study: (a) was procured from a test group animal 60 min following circulatory death; (b) from a control group animal 30 min following circulatory death. The heart in (a) shows no signs of IMC, while IMC is fully developed in (b), as seen by the severely restricted left-ventricular lumen. The average left ventricular wall thickness, measured half-way between the atrial-ventricular plane and the apex at the time of dissection, was 10 mm (range 8–16) within the test group and 20 mm (range 16–22) within the control group.

Fig. 5 shows the hemodynamic responses for all test and control subjects, following withdrawal of life-sustaining therapy at $t = 0$ min. The markers in Fig. 5a show oxygen saturation (s_aO_2) of arterial blood gas samples. The dotted horizontal line corresponds to $s_aO_2 = 30\%$. All individuals reached an arterial saturation below 30% within 3 min following WLST. The mean \pm standard deviation durations between WLST and occurrence of $s_aO_2 = 30\%$, linearly interpolated between samples, were 133 ± 38 s in the test group and 143 ± 27 s in the control group. Mean \pm standard deviation desaturation rates were -29 ± 4 %/min in the test group and -33 ± 12 %/min in the control group. This indicates similar metabolic rates between the groups. Systolic aortic pressures (P_{sys}) are shown in Fig. 5b. The dotted horizontal line corresponds to $P_{sys} = 40$ mmHg, indicating the systolic pressure associated with circulatory collapse. Heart rates (HR), computed from ECG RR-intervals until loss of QRS-complex, or onset of VF, are shown in Fig. 5c. Per-individual events are shown in the top part of Fig. 6, in which time zero corresponds to circulatory death. The bottom part visualizes the temporal distribution of events.

There was no notable overdosing of nitroglycerine in any of the cases. Consequently, the noradrenaline controller administered only very small drug doses in two cases: 1.1 μ g, beginning 149 s in T4 after WLST; 6.5 μ g

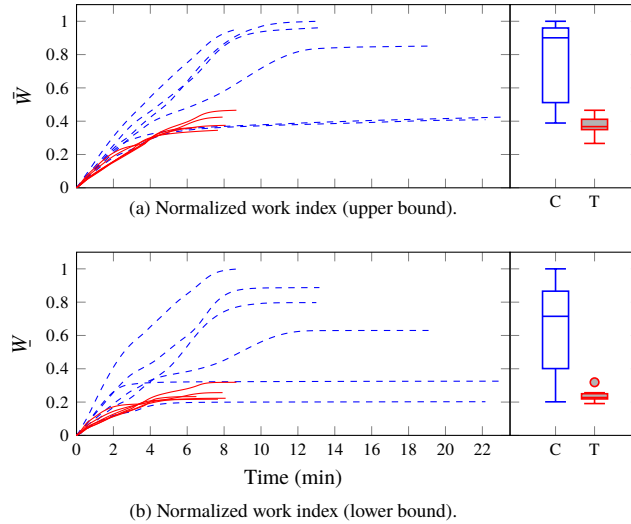


Fig. 7 Normalized work indices between withdrawal of life-sustaining therapy (WLST) at time 0 min and the incidence of either asystole or ventricular fibrillation are shown to the left. Test group estimates are shown in solid red; control group estimates in dashed blue. The two lowermost curves in the control group correspond to individuals C2 and C6 in Fig. 6, which showed circulatory collapse less than five minutes after WLST. Data computed using (1) is shown in (a) and using (2) is shown in (b). The normalized work index final value distributions of the control group (C, empty blue boxes) and test group (T, filled red boxes) are shown to the right.

in T6, beginning 113 s after WLST.

Work indices \underline{W} and \bar{W} for all individuals are shown in Fig. 7. The distributions of their final values are shown to the right in the same figure. The median decrease in work indices between control and test group was 59 % for \underline{W} and 68 % for \bar{W} .

The single-sided Mann-Whitney test reveals a significant ($p < 0.002$) difference in IMC incidence 60 min after withdrawal of life-sustaining therapy between the groups.

4 Discussion

This study demonstrated that it is feasible to postpone ischemic myocardial contraction up to 1 h following circulatory death, through automatic control of hemodynamic drug delivery.

However, further investigation needs to be undertaken to see if the asystolic non-contracted heart may be reconditioned to partial or full function after 30 min or 60 min of circulatory arrest *in situ* at normothermia. Histological comparison, *ex vivo* functional evaluation, and ultimately transplantation are markers suggested for further evaluation to determine feasibility for transplantation. A method to recondition and preserve porcine hearts has been developed in-house [17, 18]. Safe orthotopic transplantation was done with hearts extracted 24 h after brain death and kept vital by non-ischemic-heart-perfusion (NIHP) for 24 h [18]. To validate non-contracted hearts up to 1 h after circulatory death, we plan to do NIHP, followed by orthotopic transplantation. If the function of such hearts is good, this method may support broader clinical implementation of heart transplantation following withdrawal of life-sustaining therapy (controlled DCD).

While it is possible to implement the protocol manually in a controlled lab environment with well-rehearsed personnel, its clinical feasibility is low, taking into account the narrow timing requirements and the requirement of calm and dignity in the presence of next of kin. The use of a feedback control system solves both these problems. Clinical implementation relies only on standard ICU monitoring and intravenous access, both of which can be expected in the considered patient category.

The controlled DCD model used in this work is similar to the clinical scenario [19]. However, unlike the clinical scenario, the animals had not suffered neurological damage. Measures were therefore taken to establish a standardization of the agonal phase, further explained in Supplementary Sect. S3, manifested in the small variability in desaturation profiles shown in figure Fig. 5a. While the test group protocol was designed to include only drugs broadly accepted in the considered context, local protocols can affect admissibility of certain drugs. We have found no reason to believe that the test group results could not have been obtained by means of another set of drugs with similar hemodynamic effects, as long as timing and dosing are appropriately chosen.

There is no internationally recognized definition of circulatory death. It is therefore debatable whether the

definition used in this work ($s_aO_2 < 30\%$ and $P_{sys} < 40\text{ mmHg}$) would gain broad acceptance. However, the conclusion of the study would be the same with slightly differing definition of circulatory death (based on the same parameters), as can be verified by studying the profiles of Fig. 5.

As seen in Fig. 5, and reported in other preclinical studies [16, 20], the time between WLST and circulatory collapse is generally shorter than in clinic, where it is usually around 15–20 min, in absence of agonal breathing [8]. Furthermore, the circulatory collapse process progressed somewhat more rapidly in the test group. This was observed during the study, once the test and control group protocols had been fixed. In subsequent experiments we made the automated drug delivery less aggressive, and increased the systolic pressure setpoint for the noradrenaline “safety” controller during the initial phase following WLST. With these changes to the test group protocol, we were able to postpone IMC beyond 1 h with hemodynamic trajectories like those of the study controls.

The final values of the work indices in Fig. 7 and corresponding IMC onset times in Fig. 6 indicate that the work indices constitute useful predictors of IMC onset. Circulatory collapse occurred after less than five minutes in two of the control group individuals: C2 and C6 in Fig. 6. This resulted in work indices similar to those representative for the test group and a later occurrence of stone heart (37 min and 44 min). Relatedly, the distinct difference in final work indices between the control and test group shown in Fig. 7 indicates that the investigated protocol for pharmacological normalization of hemodynamics is effective in postponing the onset of IMC following WLST in the considered large animal model.

5 Conclusion

A pharmacological method, intended to postpone the onset of ischemic myocardial contracture (IMC), with the aim to facilitate controlled DCD procurement of hearts, was developed and evaluated. None of the six test group animals developed IMC within 60 min of warm ischemia, following circulatory death caused by withdrawal of life-sustaining therapy. All six control group animals developed ischemic myocardial contracture within 60 min following circulatory death, with four having developed IMC by the time of sternotomy, 30 min following circulatory death. This demonstrates pre-clinical feasibility of the proposed method, and motivates further research aimed at adapting it for the clinical setting. Further studies are needed to investigate whether the function of the heart can be fully restored.

Disclosure statement

Wahlquist, Soltesz, Liao, Liu, Pigot, Sjöberg and Steen declare that they have no conflict of interest. The work was funded by the Swedish government through the Swedish Research Council (grant 2017-04989) and the Hans-Gabriel and Alice Trolle-Wachtmeister Foundation for Medical Research. Wahlquist and Soltesz are members of the Excellence Center at Linköping-Lund in Information Technology (ELLIIT).

Animal ethics

Twelve Swedish pigs (*sus scrofa domesticus*) with a median body weight of 35 kg (range 30–40 kg) were included in the study with equal control and test group sizes of $n = 6$.

Large-animal experiments were motivated by the lack of adequate dynamic models describing the impact of pharmacological treatments on the duration to onset of IMC, or data on which such models could be based. All institutional and national guidelines for the care and use of laboratory animals were followed and approved by the appropriate institutional committees. The animals were treated in compliance with EU directive [21]. The study ran under ethics permission M174-15, issued by “Malmö/Lunds Djurförsöksetiska Nämnd” (local REB).

Human Studies/Informed Consent

No human studies were carried out by the authors for this article.

References

- [1] Cooley A, Reul J, Wukasch C. Ischemic contracture of the heart: “stone heart”. *Am J Cardiol.* 1972;29:575–577.
- [2] Hearse DJ, Garlick PB, Humphrey SM. Ischemic contracture of the myocardium: mechanisms and prevention. *Am J Cardiol.* 1977;39:986–993.
- [3] Zumbro GL, Tillman L, Bailey AO, Treasure RL. A comparison between propranolol and hypothermia in preventing ischemic contracture of the left ventricle (stone heart). *Ann Thorac Surg.* 1978;25:541–550.
- [4] Garcia-Dorado D, Gonzalez MA, Barrabes JA, et al. Prevention of ischemic rigor contracture during coronary occlusion by inhibition of $\text{Na}^+\text{-H}^+$ exchange. *Cardiovasc Res.* 1997;35:80–89.
- [5] Suntharalingam C, Sharples L, Dudley C, Bradley JA, Watson CJE. Time to cardiac death after withdrawal of life-sustaining treatment in potential organ donors. *Am J Transplant.* 2009;9:2157–2165.
- [6] Manara AR, Murphy PG, O’Callaghan G. Donation after circulatory death. *Brit J Anaesth.* 2012;108:i108–i121.
- [7] Morrissey PE, Monaco Anthony P. Donation after circulatory death: current practices, ongoing challenges, and potential improvements. *Transplantation.* 2013;97:258–264.
- [8] Messer SJ, Axell RG, Colah S, et al. Functional assessment and transplantation of the donor heart after circulatory death. *J Heart Lung Transpl.* 2016;35:1443–1452.
- [9] Dhital K, Ludhani P, Scheuer S, Connellan M, Macdonald P. DCD donations and outcomes of heart transplantation: the Australian experience. *Indian J Thorac Cardiovasc Surg.* 2020.
- [10] MacDonald P, Dhital K. Heart transplantation from donation-after-circulatory-death (DCD) donors: back to the future—evolving trends in heart transplantation from DCD donors. *J Heart Lung Transpl.* 2019;38:599–600.
- [11] Koostra G, Daemen JH, Oomen AP. Categories of non-heart-beating donors. *Transplant Proc.* 1995;27:2893–2894.
- [12] Tibballs J, Bhatia N. Transplantation of the heart after circulatory death of the donor: time for a change in law? *Med J Australia.* 2015;203:268–270.
- [13] Novitzky D, Cooper DKC, Rosendale JD, Kauffman HM. Hormonal therapy of the brain-dead organ donor: experimental and clinical studies. *Transplantation.* 2006;82:1396–1401.
- [14] Soltész K, Sturk C, Paskevicius A, et al. Closed-loop prevention of hypotension in the heartbeating brain-dead porcine model. *IEEE T Bio-med Eng.* 2017;64:1310–1317.
- [15] Soltész K, Sjöberg T, Jansson T, et al. Closed-loop regulation of arterial pressure after acute brain death. *J Clin Monit Comput.* 2018;32:429–437.
- [16] Iyer A, Chew HC, Gao L, et al. Pathophysiological trends during withdrawal of life support: implications for organ donation after circulatory death. *Transplantation.* 2016;100:2621–2629.
- [17] Qin G, Wohlfart B, Zuo L, Hu J, Sjöberg T, Steen S. Intact coronary and myocardial functions after 24 hours of non-ischemic heart preservation. *Scand Cardiovasc J.* 2020;54:59–65.
- [18] Steen S, Paskevicius A, Liao Q, Sjöberg T. Safe orthotopic transplantation of hearts harvested 24 hours after brain death and preserved for 24 hours. *Scand Cardiovasc J.* 2016;50:193–200.
- [19] Wind J, Snoeijs MGJ, Brugman CA, et al. Prediction of time of death after withdrawal of life-sustaining treatment in potential donors after cardiac death. *Crit Care Med.* 2012;40:766–769.
- [20] Niederberger P, Farine E, Raillard M, et al. Heart transplantation with donation after circulatory death: what have we learned from preclinical studies? *Circ-Heart Fail.* 2019;12.
- [21] The European Parliament . On the protection of animals used for scientific purpose. tech. rep.Council of Europe 2010. Directive 2010/63/EU.
- [22] Soltész K, Grimholt C, Skogestad S. Simultaneous design of PID controller and measurement filter by optimization *IET Control Theory A.* 2017;11:348–348.

Supplement

Prevention of ischemic myocardial contracture through hemodynamically controlled DCD

Ylva Wahlquist¹, Kristian Soltesz¹, Qiuming Liao², Xiaofei Liu³, Henry Pigot¹, Trygve Sjöberg² and Stig Steen²

¹Wahlquist, Soltesz and Pigot are with the Department of Automatic Control, Lund University, Lund, Sweden. Correspondence to Ylva Wahlquist, E-mail: ylva.wahlquist@control.lth.se

²Liao, Sjöberg and Steen are with the Division of Thoracic Surgery, Department of Clinical Sciences, Lund University, Sweden and the Department of Cardiothoracic Surgery, Skåne University Hospital, Sweden

³Liu is with the First Affiliated Hospital of Zhengzhou University, Zhengzhou, China

S1 Cardiac work estimation

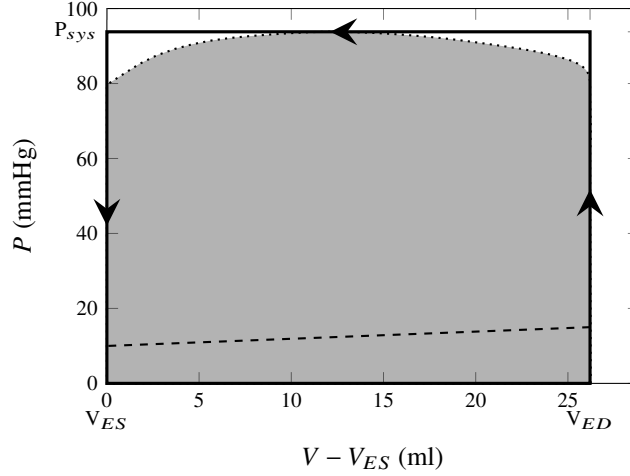


Fig. S1 Systolic pressure-volume (PV) path (dotted) between end-diastole, (ED , mitral valve closure), and end-systole, (ES , aortic valve closure), was recorded in a 30 kg pig during one pilot experiment, represented Fig. S2. The left-ventricular diastolic PV path, from ES to ED , of the cardiac cycle (dashed) is only qualitatively illustrated, and not used when considering the entire heart, rather than the isolated left ventricle. The net work performed by the left-ventricle during the cardiac cycle is the area between the dotted and dashed lines; corresponding net work performed by the heart is quantified by the grey area. The area enclosed by the solid line is the proposed cardiac cycle work estimate, \hat{W}_c , defined through (S4).

Left ventricular pressure-volume (PV) loops are frequently used in clinical and research cardiology. The PV loop shows ventricular pressure plotted against ventricular volume over one or several cardiac cycles, providing a contour similar to the one enclosing the grey area of Fig. S1. Integrating pressure over volume in the PV loop over one cardiac cycle yields the work exerted *on* the system. The work exerted *by* the system is hence

$$W(V_1, V_2) = - \int_{V_1}^{V_2} P(V) dV, \quad (\text{S1})$$

when transitioning from a volume V_1 to another volume V_2 along the PV contour. To be accurate, (S1) provides an upper bound for this work, and that bound is tight for lossless systems. This assumption is tacitly made in cardiac PV loop analysis, where the area enclosed by the PV contour is defined to be the stroke work. It is, however, not valid during ventricular fibrillation (VF), in which considerable energy is consumed without resulting in net blood transport, and hence no work is done according to (S1).

Letting t_1 be the time at which the volume is V_1 , i.e., $V(t_1) = V_1$, and similarly defining t_2 through $V(t_2) = V_2$, the work of (S1) can be expressed as

$$W(t_1, t_2) = - \int_{t_1}^{t_2} P(t) \frac{dV}{dt} dt = - \int_{t_1}^{t_2} \varphi(t) P(t) dt, \quad (\text{S2})$$

where $\varphi(t) = \dot{V}(t)$ is the volumetric flow rate entering the left ventricle. When $W > 0$, the left ventricle exerts work *on* the blood; when $W < 0$, the blood exerts work on the left ventricle. Since $P > 0$ throughout the cardiac cycle, $W > 0$ holds whenever left ventricular volume decreases ($\dot{V}(t) < 0$, characterized by the dotted line in Fig. S1), and work is exerted by the blood whenever left ventricular volume increases: $\dot{V}(t) > 0$, characterized by the dashed line in Fig. S1. The relatively small fraction of work exerted *by* the blood, quantified by the area under the dashed line in Fig. S1, can be viewed as a free contribution when the left ventricle is considered as an isolated system, which is commonly the case in PV loop analysis. However, when considering the entire heart, this contribution is not free: it is the combined contribution of the atria and the right ventricle.

Under the valid assumption that central venous pressure is low compared to aortic pressure, the work W_c , exerted by the heart during one cardiac cycle can thus be expressed

$$W_c = \int_{t_{ED}}^{t_{ES}} P(t) CO(t) dt, \quad (\text{S3})$$

where P is the (instantaneous) aortic pressure, t_{ED} the end-diastolic time instance, t_{ES} the end-systolic time instance, and $CO(t) = -\varphi$ the (instantaneous) cardiac output.

A fair approximation of W_c , \hat{W}_c , is obtained by replacing the contour segment between V_{ED} and V_{ES} with the systolic isobar in Fig. S1, P_{sys} . Then (S3) is approximated by

$$\hat{W}_c = P_{sys} SV, \quad (S4)$$

where $SV = V_{ES} - V_{ED}$ is the stroke volume. The estimate \hat{W}_c corresponds to the area enclosed by the solid line in Fig. S1. The total energy consumption between WLST and the incidence of either asystole or VF is the sum of the individual W_c contributions.

A reasonable assumption is that SV is positively correlated with P_{sys} . This will be expressed as $SV(P_{sys})$, where $SV : \mathbb{R}^+ \mapsto \mathbb{R}^+$ is some bounded monotonously non-decreasing function. The resulting relative difference in estimated work (S4) between cardiac cycles with systolic pressures P_a and $P_b < P_a$ is

$$\frac{P_a SV(P_a) - P_b SV(P_b)}{P_a SV(P_a)} = 1 - \frac{P_b SV(P_b)}{P_a SV(P_a)}. \quad (S5)$$

The properties of $SV(P_{sys})$, combined with $P_b < P_a$, yield $SV(P_b) \leq SV(P_a)$, with equality when $SV(P_{sys}) \propto 1$, i.e., when SV is not increasing with P_{sys} .

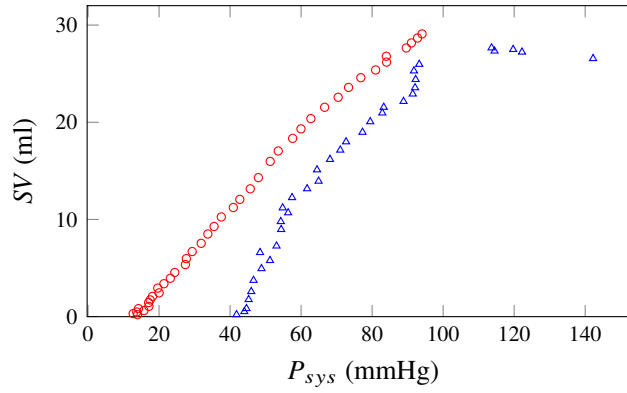


Fig. S2 Relationship between systolic aortic pressure, P_{sys} , and stroke volume, SV , measured in 30 kg animals during two pilot experiments: one illustrated by red circles; the other by blue triangles.

To justify this assumption, the nature of $SV(P_{sys})$ was investigated through two pilot experiments, where a transit-time flow meter, connected to the LabChart system detailed in Sect. S3, was secured across the aorta upon sternotomy, and otherwise adhering to the control group protocol. This enabled computing SV as the time integral of flow over each cardiac cycle. The outcome is shown in Fig. S2, confirming that the monotonicity assumption on $SV(P_{sys})$ is sound. Furthermore, it suggests that while the conservative estimate \underline{W} is accurate for the saturated region (almost horizontal segment of blue triangles), the non-saturated region (the remainder of plotted data) is better approximated by $SV(P_{sys}) \propto P_{sys}$.

A lower bound of the estimate is therefore obtained by assuming that SV is independent of P_{sys} , resulting in the total work estimate

$$\underline{W} \propto \int_0^T P_{sys}(t) HR(t) dt, \quad (S6)$$

where $t = 0$ and $t = T$ denote the instances of WLST, and asystole or VF instance, respectively. HR is the instantaneous heart rate, defined at the instances of systolic peaks as $1/\Delta t$, where Δt is the time passed since the preceding systolic peak.

The pilot experiments also suggest an upper bound on the total work estimate

$$\bar{W} \propto \int_0^T P_{sys}^2(t) HR(t) dt, \quad (S7)$$

based on SV being proportional to P_{sys} .

Since \underline{W} and \bar{W} are defined only up to proportionally, they will be denoted work *indices* rather than *estimates*, and their utility is limited to comparison between individuals or groups, within which cardiovascular physiology is similar. The central hypothesis, investigated in the study, is that the time integrals of these indices following WLST provides useful predictions of IMC incidence, and thus suggest how pharmacological normalization of hemodynamics can serve to prevent IMC.

Evaluation of the estimation of the work over one cardiac cycle (S4) of the main manuscript relies on *SV*, or equivalently *CO*, being measured. However, pilot experiments revealed that manipulation of the ischemic heart easily triggers the onset of IMC. Placement of a PV loop catheter was consequently ruled out as an option for the controlled study. Similarly, the pleural access required to place an ultra-sonic flow probe over the aorta was found to result in (partial) collapse of the lungs, suspected to affect the desaturation process. Consequently, WLST was performed with intact thorax during the study.

S2 Excluded animals and pilot cases

Three animals were excluded, all from the test group, for the following reasons: insufficient curarization resulting in agonal breathing; systolic pressure rise prior to WLST (the experiment was concluded and IMC was absent 60 min after circulatory death); nitroglycerine administration exceeding protocol limit.

In addition to the 12 included plus 3 excluded study cases, 11 pilot cases were conducted: 6 to obtain modeling data for controller design, 3 to determine adequate doses of the drugs that were not computer-controlled, and 2 to investigate the $SV(P_{sys})$ relationship explained in Supplementary Sect. S1. Pilot experiment and excluded animals fell within the same weight range as those included in the study.

S3 Study details

The animals were mechanically ventilated using volume-controlled (41 minute volume at 18 breaths/min) and pressure-regulated ventilation (5 cmH₂O PEEP). Inspired oxygen fraction was 21 %, and end tidal CO₂ was kept between 4.5 kPa and 5.5 kPa. Details of drugs and equipment used in the experiments can be found in Table S1 and S2.

Three venous catheters were secured into the superior vena cava with their tips at the level of the right atrium. These catheters were used for anesthesia maintenance, continuous venous pressure monitoring and manual drug administration. Two catheters of the same type were secured into the ascending aorta for online arterial pressure monitoring and blood gas sampling. Arterial blood gas samples were collected and analyzed at baseline, and 1, 2, . . . , 5 min following WLST.

Blood pressure transducers were connected to the arterial and venous catheters, and intermittently flushed with saline solution. Separate transducer pairs were used for the feedback control system and visualization. Both systems logged to file, results presented herein are from the LabChart logs. A 5-lead ECG was also connected to LabChart, running on a Windows 7 PC.

Rocuronium was infused at 60 mg/h, with an additional 50 mg bolus just before WLST, to prevent agonal breathing. Without complete neuromuscular blockade, one would expect a much larger spread between desaturation profiles, prompting increased study group sizes in order to draw valid comparative conclusions. Rocuronium was therefore administered to establish a neuromuscular blockade, and the endotracheal tube was clamped at the instance of WLST. Both these measures should be viewed as parts of the large-animal model, and not the proposed DCD protocol. They guarantee a total absence of gas exchange.

Bolus dose timing for the test group individuals are shown in Table S3.

Table S1: Complete list of drugs used in the main study, together with corresponding dose and manufacturer specifications. Saline solution was administered to compensate for dehydration losses.

Drug	Dose	Full drug name and manufacturer
atropine	0.5 mg	Atropin, Mylan AB, Stockholm, Sweden
esmolol	20 mg/bolus	Brevibloc, Baxter Medical AB, Kista, Sweden
heparin	25000 IU	Heparin, LEO Pharma AB, Malmö, Sweden
ketamine	750 mg	Ketaminol vet, Intervet, Boxmeer, Netherlands
lidocaine	200 mg	Xylocard, Aspen Nordic, Dublin, Ireland
midazolam	25 mg	Midazolam, Panpharma S.A, Trittau, Germany
nimodipine	0.02 mg/bolus	Nimotop, Bayer Healthcare AG, Leverkusen, Germany
nitroglycerine	1.5 mg/bolus	Nitroglycerin, BioPhausia AB, Stockholm, Sweden
noradrenaline	computer controlled	Noradrenalin, Pfizer AB, Sollentuna, Sweden
propofol	4 mg/kg/h	Propofol-Lipuro, B. Braun Medical AB, Melsungen, Germany
rocuronium	20 mg, 60 mg/h	Rocuronium, Fresenius Kabi, Graz, Austria
xylazin	100 mg	Rompun vet, Bayer AB, Solna, Sweden

Table S2: Instrumentation for measurement and drug delivery

Equipment	Name	Manufacturer
Flow meter	Flowmeter CM4000	CardioMed, Lindsay, Canada
Ventilator	Servo Ventilator 300	Siemens AB, Solna, Sweden
Venous catheter	Secalon-T	Merit Medical, Singapore
Blood gas analyzer	ABL 700	Radiometer, Copenhagen, Denmark
Blood pressure transducer	Meritans DTXPlus	Merit Medical, Singapore
DAQ	PowerLab 16/35	AD Instruments, Colorado Springs, CO
Infusion pump	Alaris TIVA	BD, Franklin Lakes, NJ
LabChart 8	AD Instruments	Colorado Springs, CO

Table S3: Bolus dose timing for test group individuals T1–T6, in seconds measured from WLST.

	Nitroglycerine			Esmolol and Nimodipine			Lidocaine, Esmolol and Nimodipine ($P_{sys} = 40$ mmHg)
	#1	#2	#3	#1	#2	#3	#1
T1	5	83	212	233			292
T2	3	81	194	216	260	292	296
T3	6			347			409
T4	177			207			350
T5	11	73					165
T6	12	126	169	192			233

S4 Nitroglycerine bolus dose

Aortic systolic pressure responses to nitroglycerine, collected during two pilot experiments, are shown in Fig. S3. The experiments indicated that a bolus dose of 1–2 mg results in a sufficient response, and that there is an apparent saturation in the vasodilative effect beyond this dose. Dose size was therefore fixed to 1.5 mg throughout the main study.

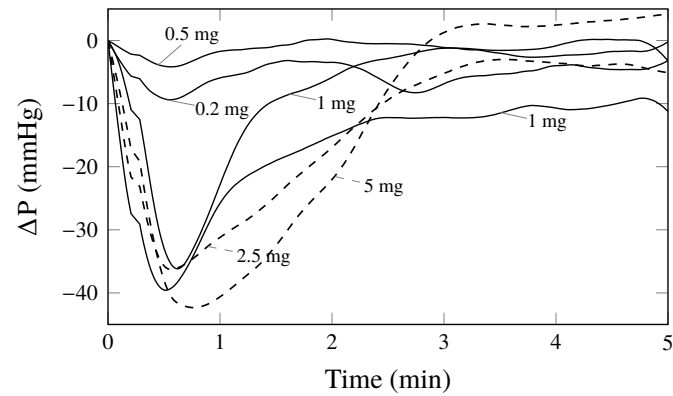


Fig. S3 Systolic pressure deviations, $\Delta P_{sys} = P_{sys} - P_0$, resulting from a nitroglycerine bolus at time zero, where P_0 denotes the baseline value of the systolic pressure P_{sys} . The responses were obtained through two pilot experiments on one 30 kg pig (dashed) and one 35 kg pig (solid).

S5 Noradrenaline controller

A noradrenaline “safety” controller was implemented for automatic drug infusion to counteract potential overdosing of nitroglycerine, otherwise resulting in hypotension. Systolic aortic pressure responses to constant noradrenaline infusions were recorded in three pilot experiments, and are shown in Fig. S4. These step responses for noradrenaline were used for identification of low-order models for the dynamics. A first-order model with time delay

$$P(s) = \frac{b}{s+a} e^{-sL} \quad (\text{S8})$$

is sufficient to describe the drug response dynamics. The model parameters a, b, L were identified by minimizing the output error \mathcal{L}_2 norm, with the error being the difference signal between measured response and corresponding model output. The resulting model parameters can be found in Table S4. A discrete time version (zero-order hold with 1 s sampling period) of the filtered PID controller was then synthesized based on a modification of the methodology in [22]. A second-order filter F was chosen to guarantee high frequency roll-off, and the filter time constant was fixed to $T_f = 2$ s, upon inspection of measurement noise characteristics in the systolic pressure signal.

The PID parameters k_p, k_i, k_d of (3) were optimized by minimizing settling time following a step output disturbance, modeling a sudden change in systolic pressure. The minimization was performed such that the maximum closed-loop 2 % settling time across the identified models was minimized. The minimization was subject to a constraint, limiting the response overshoot to 50 % of the amplitude of the disturbance step amplitude, across all identified models. This constraint was introduced to limit hypertension peaks and introduce additional robustness to the closed-loop system. The resulting optimized PID parameters were $k_p = 9.63 \cdot 10^{-4}$ mg/h/mmHg, $k_i = 2.96 \cdot 10^{-5}$ mg/h/mmHg/s, and $k_d = 8.14 \cdot 10^{-3}$ mg/h/mmHg-s.

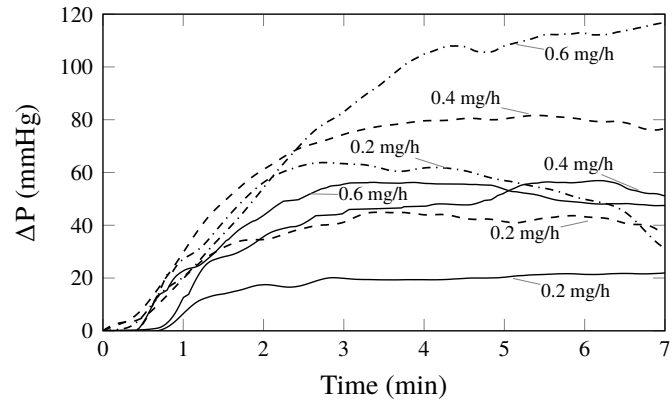


Fig. S4 Systolic pressure deviations, $\Delta P_{sys} = P_{sys} - P_0$, resulting from a noradrenaline infusion at time zero, where P_0 denotes the baseline value of the systolic pressure P_{sys} . The responses were obtained through pilot experiments using three pigs, two weighing 30 kg (solid and dashed) and one weighing 35 kg (dot-dashed)

Table S4: First order model parameters with time delay (S8), identified from noradrenaline infusion responses in Fig. S4

a	b	L
0.013	1.49	22.00
0.014	1.92	42.25
0.023	1.94	33.11
0.020	4.28	26.99
0.015	3.04	26.60
0.061	12.47	34.87
0.014	2.48	54.68